Supplemental Document

Fluid-responsive tunable metasurfaces for high-fidelity optical wireless communication

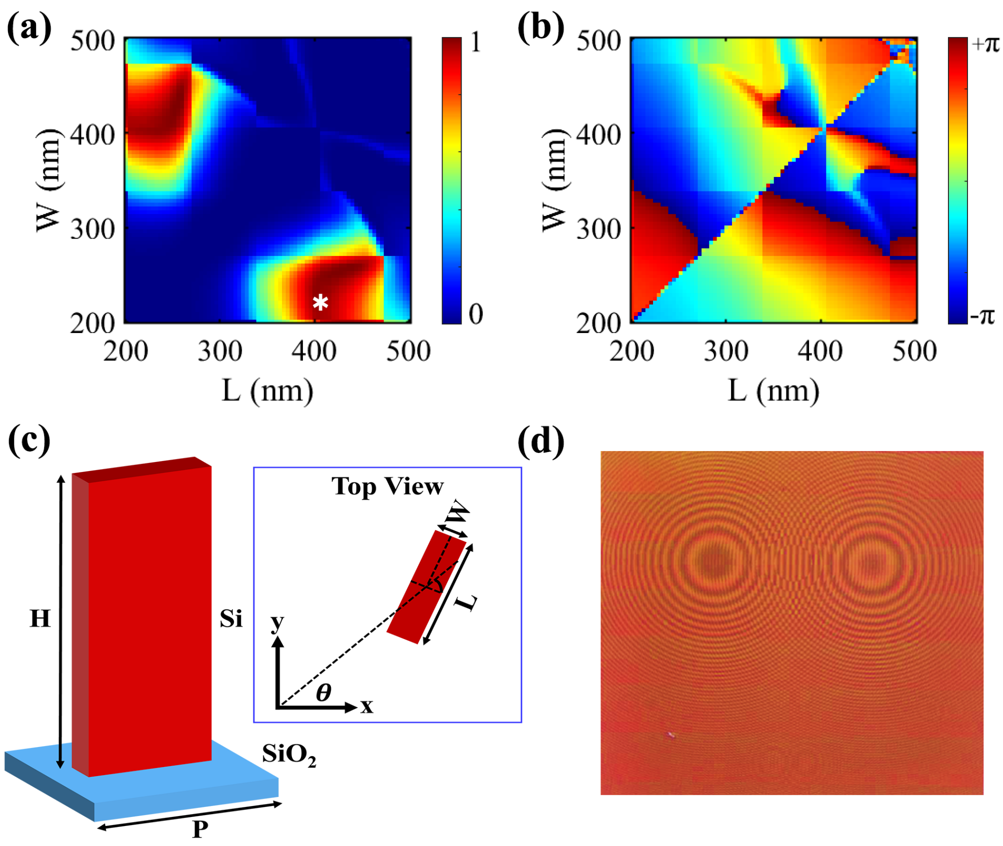

Fig. S1. Design and optimization of the unit-cell of the tunable metasurface. (a) Cross-polarized transmission plot from Length (L) vs Width (W) sweep. The steric sign depicts the selected L and W values. (b) Phase profile of the cross-polarized transmitted light. (c) Schematic of the Si-based nano-antenna. The left is the unit-cell diagram and layout schematic, and the right displays the relative positions between the center of the circle and the rotation angle of the unit-cell, where the coordinate axis means the center of the circle and the θ is the clockwise rotation angle of the unit-cell. (d) Microscopic image of the metasurface.

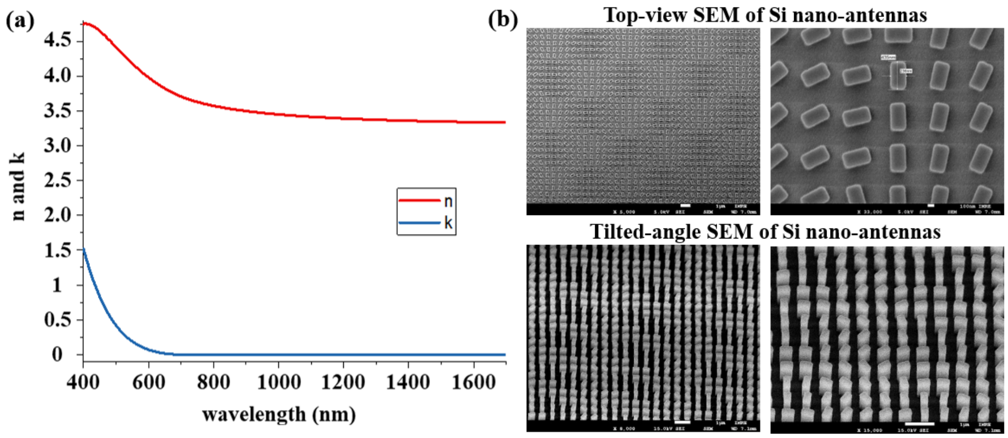

Fig. S2. Optical constants and SEM images of Si nano-antennas. (a) n and k value of Si material, and can be seen the extinction coefficient k is negligibly low at working wavelength 1550 nm and refractive index value n really high. (b) Upper SEM images representing the top-view of Si nano-antennas and lower SEM images are the tilted-angle view of Si nano-antennas.

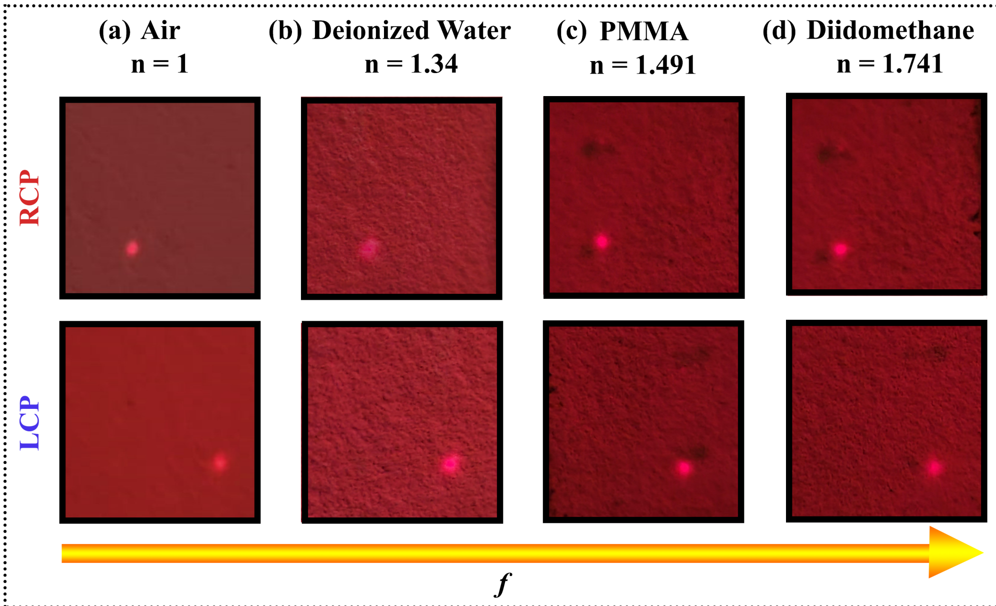

Fig. S3. Fluid-responsive tunable metasurface experimental results. (a) The focal spots (for RCP and LCP incident light) for air medium. (b) The focal spots (for RCP and LCP incident light) with deionized water. (c) The focal spots (for RCP and LCP incident light) with PMMA and (d) The focal spots (for RCP and LCP incident light) with Diidomethane. As the medium gets denser the focal length increases along the z-axis.

1. SUPPLEMENTARY NOTE. DESIGNING SPIN-ENCODED METASURFACE.

To achieve the focus of the left-circularly polarized (LCP) component, the phase profile for the metalens is formulated as follows:

$$\phi_{LCP} = +[\frac{2\pi}{\lambda}(\sqrt{x^2 + y^2 + f^2} - f)] \tag{S1}$$

Then to achieve the focus of the right-circularly polarized (RCP) component, the phase profile for the metalens is formulated as follows:

$$\phi_{RCP} = -[\frac{2\pi}{\lambda}(\sqrt{x^2 + y^2 + f^2} - f)] \tag{S2}$$

Combining the two-phase profiles is necessary to create spin-encoded metalens capable of dynamically managing photonic spin-dependent division in various dimensions, utilizing the pure geometric phase. This combined phase profile can be expressed as stated in [1].

$$\phi_{Total} = arg[e^{i\phi_{LCP}} + e^{i\phi_{RCP}}] \tag{S3}$$

2. SUPPLEMENTARY NOTE. ANALYSIS OF SI METASURFACE IN VARYING FLUID-BASED ENVIRONMENTS.

Our metasurface's wide tunability is a consequence of the substantial dispersion of several optical resonances that are induced in tandem within arrayed silicon nano-antennas. The adiabatic evolution of these optical resonances (modes) occurs when the dielectric environment is gradually altered. We use a multipole decomposition to clearly visualize the tuning of light scattering [2]. In order to project the light scattering onto the same basis when Si nano-antennas are present, analyze here [3, 4] contained in various dielectric environments. Initially, the polarization vector in silicon nano-antennas induced by the incident light is defined as in Eq. S4:

$$\mathbf{P}\left(\mathbf{r}'\right)=\varepsilon_0\left(\varepsilon_{\mathrm{Si}}-\varepsilon_{\mathrm{med}}\right)\mathbf{E}\left(\mathbf{r}'\right) \tag{S4}$$

Equation S1 depicts the polarization vector P and we have vacuum permittivity denoted by ε_0, the relative permittivity of Si denoted by $\varepsilon_{\mathrm{Si}}$, and relative permittivity of the surrounding medium denoted by $\varepsilon_{\mathrm{med}}$. The electric field distribution, denoted as $\mathbf{E}(\mathbf{r}')$, within the Si nano-antennas, can be derived from comprehensive full-field simulations. The set of polarization vectors within a particular Si nano-antennas can be expressed as a series of irreducible multipole moments in Cartesian coordinates:

$$\begin{aligned}
\mathbf{E}&=\int_\Omega \mathbf{P}\left(\mathbf{r}'\right)d\mathbf{r}'\\
\mathbf{M}&=-\frac{i\omega}{2}\int_\Omega\left[\mathbf{r}'\times\mathbf{P}\left(\mathbf{r}'\right)\right]d\mathbf{r}'\\
Q&=3\int_\Omega\left[\mathbf{r}'\mathbf{P}\left(\mathbf{r}'\right)+\mathbf{P}\left(\mathbf{r}'\right)\mathbf{r}'-\frac{2}{3}\left[\mathbf{r}'\cdot\mathbf{P}\left(\mathbf{r}'\right)\right]\right]d\mathbf{r}'\\
m&=\frac{\omega}{3i}\int_\Omega\left\{\left[\mathbf{r}'\times\mathbf{P}\left(\mathbf{r}'\right)\right]\mathbf{r}'+\mathbf{r}'\left[\mathbf{r}'\times\mathbf{P}\left(\mathbf{r}'\right)\right]\right\}d\mathbf{r}'\\
\mathbf{t}&=\frac{i\omega}{10}\int_\Omega\left\{2\mathbf{r}'^2\mathbf{P}\left(\mathbf{r}'\right)-\left[\mathbf{r}'\cdot\mathbf{P}\left(\mathbf{r}'\right)\right]\mathbf{r}'\right]\right\}d\mathbf{r}'
\end{aligned} \tag{S5}$$

The symbols E, M, and T denote the electric, magnetic, and toroidal dipole vectors, respectively, while q and m represent electric and magnetic quadrupole tensors. The complete scattering cross-section of a single Si nano-antennas can be formulated as:

$$\begin{aligned}
\sigma_{\mathrm{sca}}=&\frac{k_0{}^4}{6\pi\varepsilon_0{}^2\left|E_{\mathrm{inc}}\right|^2}\left|\mathbf{E}+\frac{ik_{\mathrm{med}}}{v_{\mathrm{med}}}\mathbf{t}\right|^2+\frac{k_0{}^4\varepsilon_{\mathrm{med}}\,\mu_0}{6\pi\varepsilon_0\left|E_{\mathrm{inc}}\right|^2}|\mathbf{M}|^2+\frac{k_0{}^6\varepsilon_{\mathrm{med}}}{720\pi\varepsilon_0{}^2\left|E_{\mathrm{inc}}\right|^2}\sum_{\alpha\beta}\left|Q_{\alpha\beta}\right|^2+\\
&\frac{k_0{}^6\varepsilon_{\mathrm{med}}{}^2\mu_0}{80\pi\varepsilon_0\left|E_{\mathrm{inc}}\right|^2}\sum_{\alpha\beta}\left|M_{\alpha\beta}\right|^2
\end{aligned} \tag{S6}$$

Due to the inherent irreducibility of these multipoles, any optical interaction between them is absent. Nonetheless, when nano-antennas assemble into a dense array characterized by a sub-wavelength period, all the scattered light is compelled to emit into two distinct optical channels, namely symmetric and anti-symmetric outgoing plane waves. Consequently, this leads to the interference of light emitted by the various multipoles.

In this study, we analyze the interference among scattered plane waves from various multipoles to reconstruct the transmission and reflection spectra of Si nano-antennas, referred to as Si metasurface. The investigation focuses on normally incident, linearly polarized (x-polarized) plane wave illumination. The expression for the total scattered light from a single Si nano-antenna in the direction perpendicular to the metasurface plane is provided as in Eq. (S7):

$$E_{sca_E,F(B)}=\frac{k_0{}^2e^{ik_{\mathrm{med}}r}}{4\pi\varepsilon_0 r}\left(E_x+\frac{ik_{\mathrm{med}}}{v_{\mathrm{med}}}t_x+(-)\frac{1}{v_{\mathrm{med}}}M_y-(+)\frac{ik_{\mathrm{med}}}{6}Q_{xz}-\frac{ik_{\mathrm{med}}}{2v_{\mathrm{med}}}m_{yz}\right) \tag{S7}$$

Here, $E_{sca_E,F(B)}$ denote the scattered light in the forward and backward directions, respectively. k_{med} and v_{med} represent the wavevector and speed of light in the surrounding medium, and r signifies the distance between the field point and the source point.

We establish $E(H)_{sca,F(B)}$ as the electric (magnetic) field of scattered plane waves originating from a metasurface in the forward (backward) direction. Conceptually, the scattered plane waves from a Huygens' metasurface can be correlated with hypothetical electric (J_s) and magnetic (m_s) surface current density, artificially introduced at the interface to fulfill the boundary conditions:

$$J_{\mathrm{s}} = H_{\mathrm{sca,B}} - H_{\mathrm{sca,F}}; \quad M_{\mathrm{s}} = E_{\mathrm{sca,F}} - E_{\mathrm{sca,B}} \tag{S8}$$

So it can be written that the contribution to (J_s) from the electric dipole moment is defined as in Eq. (S9):

$$J_{\mathrm{s},p_x} = \frac{\partial P}{\partial t} = \frac{-i\omega E_x}{a^2} \tag{S9}$$

In above Eq. (S9), a is the length of the nano-antenna of the metasurface.

$$\begin{aligned}
J_{\mathrm{s}} &= \frac{-i\omega}{a^2}\left(E_x + \frac{ik_{\mathrm{med}}}{v_{\mathrm{med}}} t_x - \frac{ik_{\mathrm{med}}}{2v_{\mathrm{med}}} m_{yz}\right) \\
m_{\mathrm{s}} &= \frac{i\omega}{a^2}\sqrt{\frac{\mu_0}{\varepsilon_0 \varepsilon_{\mathrm{med}}}}\left(\frac{1}{v_{\mathrm{med}}} M_y - \frac{ik_{\mathrm{med}}}{6} Q_{xz}\right) \\
E_{\mathrm{sca,F}} &= E_{\mathrm{sca,sym}} + E_{\mathrm{sca,anti}} \\
E_{\mathrm{sca,\,B}} &= E_{\mathrm{sca,sym}} - E_{\mathrm{sca,anti}}
\end{aligned} \tag{S10}$$

$$\begin{aligned}
E_{\mathrm{sca,sym}} &= \frac{ik_{\mathrm{med}}}{2a^2 \varepsilon_0 \varepsilon_{\mathrm{med}}}\left(E_x + \frac{ik_{\mathrm{med}}}{v_{\mathrm{med}}} t_x - \frac{ik_{\mathrm{med}}}{2v_{\mathrm{med}}} m_{yz}\right) \\
E_{\mathrm{sca,anti}} &= \frac{ik_{\mathrm{med}}}{2a^2 \varepsilon_0 \varepsilon_{\mathrm{med}}}\left(\frac{1}{v_{\mathrm{med}}} M_y - \frac{ik_{\mathrm{med}}}{6} Q_{xz}\right)
\end{aligned} \tag{S11}$$

$$t = \left|E_{\mathrm{inc}} + E_{\mathrm{sca,sym}} + E_{\mathrm{sca,anti}}\right|^2; \quad R = \left|E_{\mathrm{sca,sym}} - E_{\mathrm{sca,anti}}\right|^2 \tag{S12}$$

In line with Eq. (S12), achieving amplitude control necessitates precise alignment between (S_s) and (S_a) for the "off" state and minimal overlap for the "on" state. Additionally, we make the assumption that the metasurface is lossless $\gamma_{ds} = \gamma_{da} = 0$. The intended dispersive behavior is outlined as follows:

$$\begin{aligned}
\lambda_{\mathrm{s}}(n) &= \left[0.9 + \frac{3}{14}(n-1)\right]\lambda_{\mathrm{d}} \\
\lambda_{\mathrm{a}}(n) &= \left[0.95 + \frac{1}{7}(n-1)\right]\lambda_{\mathrm{d}} \\
Q_{\mathrm{s}}(n) &= 30 - \frac{100}{7}(n-1) \\
Q_{\mathrm{a}}(n) &= 10 + \frac{100}{7}(n-1)
\end{aligned} \tag{S13}$$

REFERENCES

1. M. A. Ansari, I. Kim, D. Lee, M. H. Waseem, M. Zubair, N. Mahmood, T. Badloe, S. Yerci, T. Tauqeer, M. Q. Mehmood *et al.*, "A spin-encoded all-dielectric metahologram for visible light," Laser & Photonics Rev. **13**, 1900065 (2019).
2. Q. Li, J. van de Groep, A. K. White, J.-H. Song, S. A. Longwell, P. M. Fordyce, S. R. Quake, P. G. Kik, and M. L. Brongersma, "Metasurface optofluidics for dynamic control of light fields," Nat. Nanotechnol. **17**, 1097–1103 (2022).
3. A. B. Evlyukhin, T. Fischer, C. Reinhardt, and B. N. Chichkov, "Optical theorem and multipole scattering of light by arbitrarily shaped nanoparticles," Phys. Rev. B **94**, 205434 (2016).
4. P. D. Terekhov, V. E. Babicheva, K. V. Baryshnikova, A. S. Shalin, A. Karabchevsky, and A. B. Evlyukhin, "Multipole analysis of dielectric metasurfaces composed of nonspherical nanoparticles and lattice invisibility effect," Phys. Rev. B **99**, 045424 (2019).